2004

Anomalous temperature-dependent transport in YbNi2B2C and its correlation to microstructural features

M.A. Avila
Iowa State University

Y.Q. Wu
Iowa State University

C.L. Condron
Iowa State University

Sergey L. Bud'ko
Iowa State University, budko@ameslab.gov

M. J. Kramer
Ames Laboratory (DOE), mjkramer@ameslab.gov

Follow this and additional works at: http://lib.dr.iastate.edu/chem_pubs

Part of the Biological and Chemical Physics Commons, Materials Chemistry Commons, Other

See next page for additional authors

Materials Science and Engineering Commons, and the Physical Chemistry Commons

The complete bibliographic information for this item can be found at http://lib.dr.iastate.edu/ chem_pubs/853. For information on how to cite this item, please visit http://lib.dr.iastate.edu/ howtocite.html.

Anomalous temperature-dependent transport in YbNi2B2C and its correlation to microstructural features

Abstract

We address the nature of the ligandal disorder leading to local redistributions of Kondo temperatures, manifested as annealing-induced changes in the transport behavior of the heavy fermion system YbNi2B2C. The anomalous transport behavior was fully characterized by temperature dependent resistivity measurements in an extended range of 0.4

Disciplines

Biological and Chemical Physics | Materials Chemistry | Other Materials Science and Engineering | Physical Chemistry

Comments

Authors

M.A. Avila, Y.Q. Wu, C.L. Condron, Sergey L. Bud'ko, M. J. Kramer, Gordon J. Miller, and Paul C. Canfield

Anomalous temperature-dependent transport in YbNi₂B₂C and its correlation to microstructural features

M. A. Avila,[1,2] Y. Q. Wu,[1,3] C. L. Condron,[1,4] S. L. Bud'ko,[1] M. Kramer,[1,3] G. J. Miller,[1,4] and P. C. Canfield[1,2]

[1]*Ames Laboratory, Iowa State University, Ames, Iowa 50011, USA*
[2]*Department of Physics and Astronomy, Iowa State University, Ames, Iowa 50011, USA*
[3]*Department of Materials Science and Engineering, Iowa State University, Ames, Iowa 50011, USA*
[4]*Department of Chemistry, Iowa State University, Ames, Iowa 50011, USA*

We address the nature of the ligandal disorder leading to local redistributions of Kondo temperatures, manifested as annealing-induced changes in the transport behavior of the heavy fermion system YbNi₂B₂C. The anomalous transport behavior was fully characterized by temperature dependent resistivity measurements in an extended range of $0.4 < T < 1000$ K for as-grown and optimally annealed single crystals, and microstructural changes between these two types of samples were investigated by single-crystal x-ray diffraction and transmission electron microscopy. Our results point to lattice dislocations as the most likely candidate to be affecting the surrounding Yb ions, leading to a distribution of Kondo temperatures. This effect combined with the ability to control defect density with annealing offers the possibility of further understanding of the more general problem of the enhanced sensitivity of hybridized Kondo states to disorder, particularly above the coherence temperature.

I. INTRODUCTION

The transport properties of heavy fermion intermetallic systems often display peculiar behaviors[1] whose origin remains as yet unestablished and are subject of current interest. In these systems the effective mass of conduction electrons is enhanced as a result of hybridization between localized electronic orbitals and delocalized conduction bands, and apparently these hybridized states tend to be particularly sensitive to crystalline disorder, manifesting strong sample-to-sample variations in the transport properties[1,2] which go beyond trivial differences in residual resistivity.

The quaternary compound YbNi₂B₂C is a ytterbium-based heavy fermion[3,4] with an electronic specific heat coefficient, $\gamma \approx 500$ mJ/mol K², and a Kondo temperature, $T_K \approx 10$ K: a temperature scale that is well separated from any other characteristic temperatures since no superconducting or magnetic transitions were found above 0.03 K, and the first crystal electric field excited level is ≈ 100 K.[3–7] This compound is therefore favorable for the study of Kondo physics. Furthermore, an investigation of the effects of annealing on the resistive behavior of boro-carbide single crystals[8] found that YbNi₂B₂C displayed radical changes in temperature-dependent resistance below room temperature, pointing to the possibility that the transport properties of this compound could be "tuned" to a certain extent by annealing, and thus offer a model system to study the relationship between disorder and hybridized states near the Fermi level.

In a previous report,[9] we demonstrated a significant variation in the temperature-dependent electrical resistivity (2–300 K) and thermoelectric power (90–310 K) between as-grown crystals and crystals that had undergone annealing at 950 °C, whereas the thermodynamic properties (heat capacity and magnetic susceptibility between 2–300 K) remained almost unchanged. We interpreted these results in terms of redistributions of local Kondo temperatures associated with ligandal disorder for a small (on the order of 1%) fraction of the Yb sites. This hypothesis left open two obvious questions: (i) What happens to the electrical resistivity for temperatures greater than the maximum possible T_K in this proposed distribution? and (ii) What is the microscopic origin of this distribution of Kondo temperatures?

In the present work, we first extend the temperature range of resistivity measurements both higher (up to 1000 K) and lower (down to 0.4 K), in order to fully characterize the transport behavior of as-grown and optimally annealed crystals and provide further evidence of the proposed model. We then present x-ray single-crystal refinements and transmission electron microscopy experiments, which provide new information on the types of disorder that may be causing the anomalous Kondo temperatures in the surrounding Yb sites. The results of this study further support our hypothesis and clearly establish YbNi₂B₂C as a rare example of a heavy Fermion compound in which characterizable structural disorder can be tuned and clearly associated with conspicuous changes in the electrical transport properties.

II. EXPERIMENTAL DETAILS

Single crystals of YbNi₂B₂C were grown by the flux method using Ni₂B flux.[3,10] For the resistivity measurements, a particularly clean and well-formed single crystal plate measuring approximately $7 \times 3 \times 0.2$ mm³ was selected, polished on both surfaces to remove most of the attached flux, and cut using a wire saw into flat bars of typical dimensions $2 \times 0.5 \times 0.13$ mm³ with the longest length parallel to the [100] direction. Electrical contacts were placed on three unannealed samples in 4-probe linear geometry by attaching Pt wires to a sample surface with Ablebond 88-1 silver epoxy. The weight and dimensions of each sample was carefully measured and the resulting sample densities (8.3
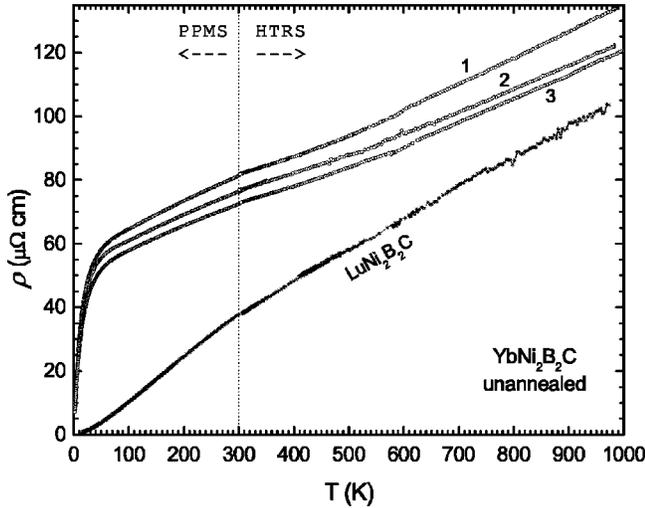
FIG. 1. Temperature dependence of the electrical resistivity of three unannealed pieces of $YbNi_2B_2C$ cut from the same crystal. The differences between these curves are within an uncertainty of 10% in estimating the sample geometry. A crystal of $LuNi_2B_2C$ was also measured as a reference for the conventional electron-phonon contribution to scattering.

FIG. 2. Temperature dependence of the electrical resistivity of two pieces of $YbNi_2B_2C$ cut from the same crystal, before and after annealing at 950 °C for 150 h. The measurement on $LuNi_2B_2C$ serves as a reference for the standard electron-phonon contribution to scattering.

± 0.2 g/cm^3) allow us to estimate an upper limit of $\pm 10\%$ for the overall uncertainty in calculating resistivity $\rho = RA/d$, where A is the cross-sectional area and d is the distance between voltage leads.

Two measured samples were then selected to undergo annealing for comparison. The Pt wires were removed and the silver epoxy was polished off, leading to a small ($\sim 10\%$) decrease in the sample's original weight due to an intentional, slight overpolishing. Since the polishing occurred on a single flat surface parallel to the current direction, the reduction in the sample cross section was assumed to be the same as the one in mass. The samples were then annealed in vacuum for 150 hours at 950 °C (details of the annealing procedure are described in Ref. 9).

Electrical resistance measurements below room temperature were performed on commercial Quantum Design PPMS systems, allowing measurements down to 1.8 K, or down to 0.4 K if the ^{3}He option is installed. Above room temperature, measurements were performed on a custom-built high temperature resistivity system (HTRS) which can be mounted on the same system used for sample annealing under vacuum ($\sim 10^{-6}$ Torr). A quartz probe is inserted in the system with four leads where the other end of the sample contacts are attached using silver epoxy. Temperature is measured with two independent thermometers: Pt resistance temperature detector (RTD) and type-R thermocouple. A 1 mA current is applied on the sample by a Keithley 220 current source and the voltage is read on a HP 34420A nanovoltmeter. The RTD current is applied by a LakeShore 120 current source and the voltage is read on a HP 34401A multimeter. The thermocouple voltage is read by another HP 34420A nanovoltmeter. All these instruments are GPIB interfaced with a computer running a custom-made software for data acquisition. To reduce noise and avoid diode or thermoelectric effects, five readings are taken with the current in each
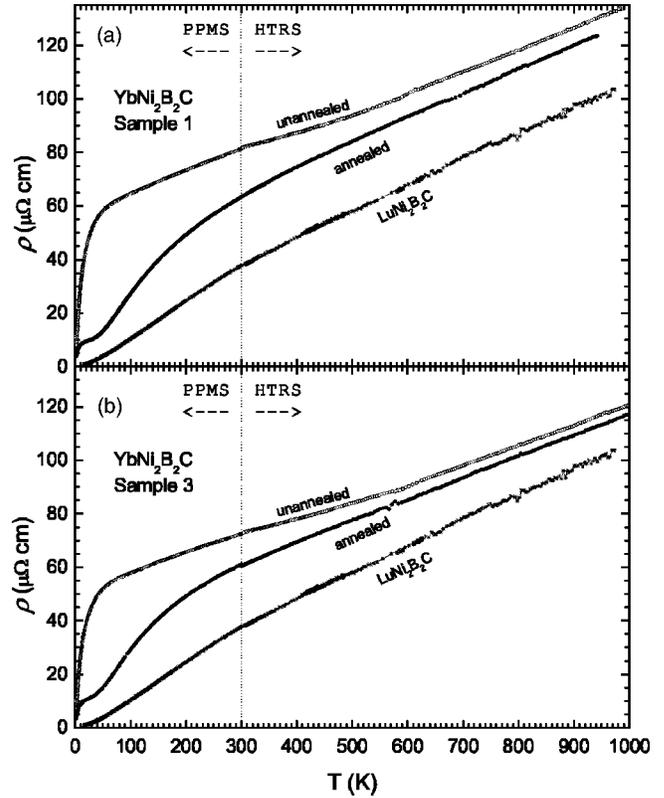
direction, and the ten absolute voltage values are averaged.

A typical HTRS experiment proceeds as follows. (1) The system is heated to 450 K for about an hour in air to cure the contacts, then cooled back to room temperature. (2) The vacuum system is turned on and allowed to achieve a dynamic vacuum of 10^{-5} Torr or better. (3) The furnace temperature is ramped at 2 K/min or slower up to about 600 K and back to room temperature, while the software acquires data points every 2 min. This first ramp is used to allow further stabilization of the contacts which often undergo small changes when heated, marked by irreproducible shifts in the resistance behavior. (4) The definitive dataset is acquired by ramping at 2 K/min or slower up to about 1000 K and back to room temperature, while the software acquires data points every 2 min. For the same reason of contact stability and in order to obtain a good match between the curves from both measurement systems, the low temperature measurements in the PPMS were performed only after the high temperature ones, and for each sample the data presented in Figs. 1 and 2 is the cool down from 1000 K to 300 K in the HTRS, followed by the cool down from 300 K to 1.8 K or 0.4 K in the PPMS. A certain level of mismatch still remains at room temperature, both for the absolute value of the measured resistance and for its slope, but these differences are considered small enough to be neglected in the comparative analysis we present in this work.

For the crystallographic studies, room temperature x-ray diffraction (XRD) data of as-grown and annealed $YbNi_2B_2C$ single crystals were collected using a Bruker APEX diffractometer with Mo $K\alpha$ radiation ($\lambda = 0.710\,73$ Å) and a detector-to-crystal distance of 5.08 cm. Data were collected for the full sphere and were harvested by collecting three sets of frames with 0.3° scans in ω for an exposure time of 10 seconds per frame. The range of 2θ extended from 3.0° to 56.0°. Data were corrected for Lorentz and polarization effects; absorption corrections were based on fitting a function to the empirical transmission surface as sampled by multiple equivalent reflections. Unit cell parameters were indexed by peaks obtained from 90 frames of reciprocal space images and then refined using all observed diffraction peaks after data integration. Together with systematic absences, the space group $I4/mmm$ (N. 139) was selected for subsequent structural analysis. The structure solution was obtained by direct methods and refined by full-matrix least-squares refinement of F_o^2 using the SHELXTL 6.10 package.[11]

For the transmission electron microscopy (TEM) evaluations, the as-grown and annealed single crystals of $YbNi_2B_2C$ were characterized using a Philips CM30 transmission electron microscope operating at 300 keV. The single crystals were placed in a mortar with denatured ethyl alcohol and ground to a fine powder. A pipette was used to place a small drop of the suspension onto a holey carbon grid. The suspension was air-dried before insertion into the microscope. The crystalline structure of fragments which were electron transparent was evaluated using selected area electron diffraction pattern (SADP). The defect density was measured on select areas of the bright-field images where the thickness was relatively uniform.

III. RESISTIVITY MEASUREMENTS

The main motivation for extending the resistivity measurements to high temperatures was based on the assumption that, if the excess scattering seen at room temperature and below in unannealed samples arises from the contribution of Yb sites with Kondo temperatures extending up through room temperature, there should be a temperature T_K^{max} above which the samples no longer display anomalous scattering, and the difference between the resistivity of unannealed sample and the annealed sample becomes a "simple" Matthiessen impurity term.

The temperature dependence of the electrical resistivity for three unannealed pieces of $YbNi_2B_2C$ cut from the same crystal is shown in Fig. 1. The general behavior below room temperature is the same as has been previously reported for as-grown samples of this compound,[8,9,12–15] i.e., a high-scattering metallic behavior down to about 30 K, below which the resistivity decreases rapidly. If normalized to their respective resistance values at any given temperature, these three curves essentially collapse into a single one in the entire measured temperature interval, meaning that the selected crystal was quite homogeneous and the differences seen in the three measurements result from the overall ±10% uncertainty in estimating the geometrical factor A/d for each piece. The residual resistivity ratio [defined as $R(300)/$ $R(1.8)$] is $RRR = 10$ for all three samples, somewhat higher than $RRR = 6-7$ found for several other unannealed crystals grown similarly,[8,9] indicating that by measuring the high temperature region first we are already annealing out a small portion of the disorder, but still maintaining most of the characteristic unannealed sample behavior.

A crystal of $LuNi_2B_2C$ was also measured to provide a reference for the nonmagnetic (e.g., standard electron-phonon) contribution to scattering down to 16 K, below which it becomes superconducting. The high temperature region is somewhat noisier for this sample because its cross section is about $3\times$ larger than the others and therefore the actual measured resistance is proportionally smaller. On the other hand, the uncertainty in this sample's geometrical factor is equally smaller, so its slope becomes a good reference. It is interesting to note that, assuming $\rho_0 l = 412$ $\mu\Omega$ cm Å for $LuNi_2B_2C$,[16] near 1000 K the measured resistivity of order 100 $\mu\Omega$ cm implies a mean free path $l \sim 4$ Å, already comparable to the unit cell lattice parameter a (the Ioffe-Regel criterion); however, the resistivity behavior is still quite linear with a slope $\Delta\rho/\Delta T = 0.1$ $\mu\Omega$ cm/K between 600 K and 900 K. Above 600 K, all three $YbNi_2B_2C$ samples change slope and roughly follow that of the $LuNi_2B_2C$ sample (except for the nearly constant extra magnetic contribution).

Samples 1 and 3 were then annealed for 150 h at 950 °C and remeasured. Figures 2(a) and 2(b) present the comparison between unannealed and annealed resistivity for each sample. Let us go through the comparison in detail for sample 1. At high temperatures (above about 600 K), the curves for the unannealed and annealed conditions of the sample run essentially parallel to each other (and roughly parallel to $LuNi_2B_2C$), meaning that in this region there is simply a temperature-independent resistivity factor ρ_0, in accordance with Matthiessen's rule. As we cool below 600 K the unannealed curve maintains a more slowly decreasing resistivity (or, conversely, a *relatively* increased level of scattering), when compared to the other two which continue to run parallel down to about 200 K. Around this temperature the annealed $YbNi_2B_2C$ curve presents a broad shoulder, most likely related to the thermal depopulation of the CEF multiplet with $T_{cef} \approx 100$ K, and therefore approaches the $LuNi_2B_2C$ curve. Between 50 K and 10 K the resistivity of the annealed sample resembles a Kondo-minimum type behavior, and below 10 K its resistivity once again drops rapidly due to the onset of coherent scattering of the Yb ions, making its final approach towards the conventional scattering level of the normal-state, nonmagnetic $LuNi_2B_2C$. Qualitatively similar results are found for sample 3. For both $YbNi_2B_2C$ samples RRR increased to 17 with annealing, consistent with the previous results from annealed crystals.[9]

Following the encouraging results above, we remeasured these samples in the PPMS with the ^{3}He option in order to extend the resistivity curves down to our lowest measurable temperatures, so as to check how annealing affects the behavior in this regime and verify whether or not they follow the theoretical predictions for a Fermi liquid.

In Fig. 3(a) we show the temperature dependence of resistivity below 30 K of sample 2 which was left unannealed,
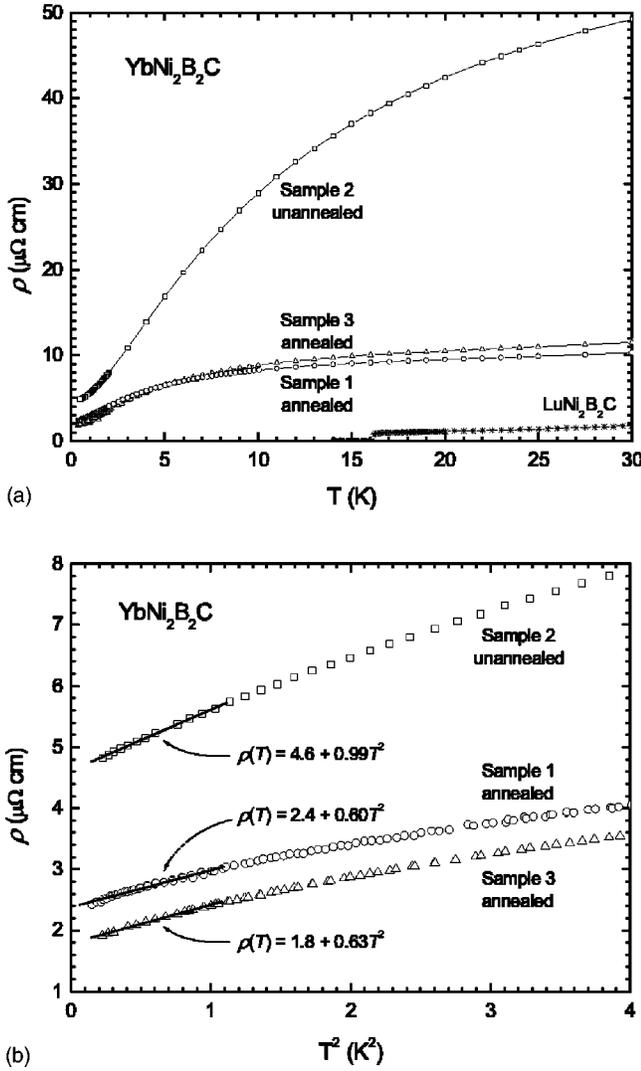
FIG. 3. (a) Low temperature region of resistivity for unannealed (sample 2) and annealed (samples 1 and 3) $YbNi_2B_2C$. $LuNi_2B_2C$ serves as comparison until it becomes superconducting at 16 K. (b) T^2 dependence of the resistivity for the $YbNi_2B_2C$ samples at the lowest measured temperatures.

and samples 1 and 3 (annealed). The decrease in resistivity below 10 K is quite evident in the annealed samples, whereas the resistivity of the unannealed one is already decreasing rapidly below 30 K. In Fig. 3(b) we plot the same data in the region below 2 K as a function of T^2, and all three curves are slightly sublinear in this plot, indicating that they cannot be completely described by a Fermi-liquid type relation $\rho(T) = \rho_0 + AT^2$ in this temperature range. In the graph we have included a fit of this expression to the three data sets below 1 K. It seems that with the decrease in disorder there is a decrease in both ρ_0 and A. The only other investigations of this type previously reported on an unannealed crystal[14,17] resulted in $\rho(T) = 12 + 1.2T^2$ $\mu\Omega$ cm, and are consistent with this trend. Such a large reduction in A is not expected within the framework of the Fermi-liquid models, since our previous study[9] found that the electronic specific heat coefficient γ changes very little with annealing (no more than 10% for the lowest measured temperatures). Even taking into account this small change in γ, the ratio A/γ_0^2 still decreases from 0.4×10^{-5} to 0.3×10^{-5} $\mu\Omega$ cm $(mol\ K/mJ)^2$ with annealing. These values are smaller than the Kadowaki-Woods ratio[18] of 1×10^{-5} $\mu\Omega$ cm $(mol\ K/mJ)^2$ found empirically for many Fermi-liquid systems, but examples of such low values like this are not unknown and have recently been compiled by Tsujii *et al.*[19] who observed that many of these "exceptions" tend to group around the ratio of 0.4×10^{-5} $\mu\Omega$ cm $(mol\ K/mJ)^2$.

The difference of $2-3$ $\mu\Omega$ cm in ρ_0 between our annealed and unannealed $YbNi_2B_2C$ samples is similar to the results obtained by annealing studies on non-hybridizing $TmNi_2B_2C^{20}$ and also comparable to the results of $Lu(Ni_{1-x}Co_x)_2B_2C$ substitution studies[16] when $x \approx 1\%$. These similarities suggest that the optimal annealing of single crystals grown by the Ni_2B flux growth method is essentially removing lattice imperfections on the order of 1%, and in the coherent scattering regime $YbNi_2B_2C$ behaves like all other members of the family. Furthermore, the difference in resistivity between annealed and unannealed samples above 600 K (Fig. 2) was found to be $3-6$ $\mu\Omega$ cm, which is remarkably similar as well (considering that the separations between the resistivity curves are strongly affected by geometrical uncertainties at these high temperatures) and therefore once again points to the return of a more conventional scattering regime at very high temperatures.

Given the consistency of the extended transport measurements with the hypothesis that ligandal disorder in the as-grown samples is leading to redistributions of Kondo temperatures for a small fraction of the Yb sites, the question that arises naturally is: what are the types of disorder contributing to this behavior? To address this question, we now present a series of structural and microscopic experiments conducted on as-grown and annealed single crystals.

IV. SINGLE CRYSTAL X-RAY REFINEMENTS

The single-crystal XRD technique is useful to check for vacancies, substitutions, superstructures, and other perturbations of periodic atomic sites in the crystal. The structure refinement for the as-grown and annealed $YbNi_2B_2C$ was carried out under the assumption that no structural disorder was present. By this assumption all systematic absences pointed to the expected[21] crystal system (tetragonal) and space group ($I4/mmm$) represented in Fig. 4. Atomic positions were assigned based on site symmetry and bond length and agree with previously published single crystal data for other RNi_2B_2C series members.[22] However, subtle problems with the initial structure refinement of the as-grown samples implied that the solution was not complete.

For most crystal structure refinements a parameter is added to account for the accordance of extinction. In the SHELXTL software the extinction parameter accounts for both primary and secondary extinction.[11] Before the extinction parameter was added to the refinement of the as-grown $YbNi_2B_2C$ the R-index was 0.1224 and the thermal parameters for Yb and B were not convergent (Table I). After the extinction parameter was added the refinement appeared to be stable with the exception of the C thermal parameter (this
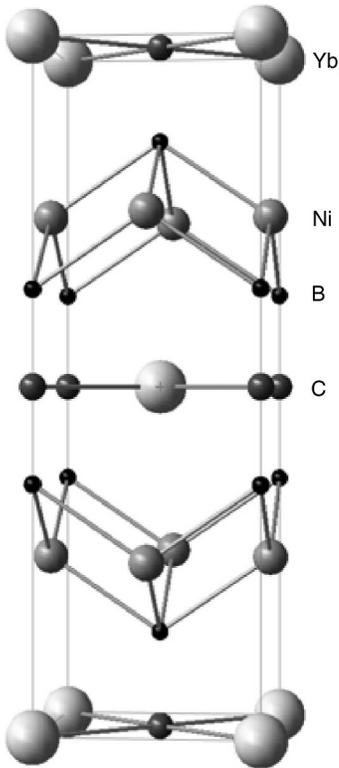
FIG. 4. Unit cell diagram of YbNi$_2$B$_2$C.

is typical for light elements in the presence of heavy elements). However, the extinction parameter itself [0.24(2)] is larger than what is normally expected (Table II). In solid state structures a large extinction parameter usually indicates the existence of a supercell structure. Because supercell structural solutions were not found in this case, as indicated by the absence of additional reflections, the large extinction parameter is most likely due to the presence of dislocations. Refinement of the annealed YbNi$_2$B$_2$C structure presented no problems [extinction parameter 0.065(8)], suggesting that much of the disorder present in the sample before the annealing process has been removed (see Table III). There is no evidence of vacancies or substitutions within the resolution limit of this technique.

V. TRANSMISSION ELECTRON MICROSCOPY

In order to obtain a more detailed and quantitative estimate of these dislocations we studied the TEM patterns of

TABLE I. As-grown YbNi$_2$B$_2$C without extinction parameter. Space group $I4/mmm$, $a = 3.479(5)$ Å, $c = 10.617(2)$ Å, $Z = 2$, $R = 0.1224$, $R_\omega = 0.222$, 558 independent reflections, 66 observed [$I > 2\sigma(I)$], 6 parameters.

Atom	x	y	z	U_{iso}
Yb	0	0	0	0.000 01
Ni	0	0.5	0.25	0.002 58(1)
B	0	0.5	0.360(7)	0.000 01
C	0.5	0.5	0	0.009 17(1)

TABLE II. As-grown YbNi$_2$B$_2$C with extinction parameter. Space group $I4/mmm$, $a = 3.487(5)$ Å, $c = 10.617(2)$ Å, $Z = 2$, $R = 0.0205$, $R_\omega = 0.0482$, extinction coefficient 0.24(2), 558 independent reflections, 66 observed [$I > 2\sigma(I)$], 7 parameters.

Atom	x	y	z	U_{iso}
Yb	0	0	0	0.0076(7)
Ni	0	0.5	0.25	0.0066(6)
B	0	0.5	0.360(7)	0.0061(3)
C	0.5	0.5	0	0.00001

crushed crystals. Figures 5(a) and 5(b) show two representative bright field TEM images and the corresponding SADPs (insets) of the crushed as-grown and annealed YbNi$_2$B$_2$C single grains, respectively. Both SADP's are fully consistent with the known space group [$I4/mmm$ (139)] for this compound, and they do have a common reciprocal lattice vector, (110), which is approximately equal for these two samples. There are no obvious second phases and the diffraction spots are sharp, indicating well crystallized samples. However, the as-grown crystallites show a surprisingly large number of dislocations [Fig. 5(a)]. In contrast, the annealed samples while exhibiting some regions of moderate defect density, the defect density is qualitatively lower than the as-grown sample. Using an estimated thickness of 800 and 500 nm for the as-grown and annealed samples, we estimate a defect density of 1.5×10^8 and $< 6 \times 10^7$ cm^{-2} for the as-grown and annealed samples, respectively.

Although it is not expected that room temperature crushing of a nominally brittle intermetallic would result in extensive dislocation formation, it is not without precedence.[23] The difference in the dislocation density between the as-grown and annealed samples may be due to the presence of Frank-Read sources, small defects which when subjected to high shear stresses are capable of overcoming the Peierls forces resisting dislocation mobility. This would imply that the as-grown crystals may have many small and hard to detect defects which are eliminated by annealing.

VI. DISCUSSION

In our previous study[9] we made a semiquantitative evaluation of the fraction of Yb sites that would need to be perturbed in order to account for the excess resistivity seen at room temperature and below in the unannealed samples. The expression describing the increase of resistivity due to a

TABLE III. Annealed YbNi$_2$B$_2$C. Space group $I4/mmm$, $a = 3.487(5)$ Å, $c = 10.643(2)$ Å, $Z = 2$, $R = 0.0266$, $R_\omega = 0.0612$, extinction coefficient 0.065(8), 929 independent reflections, 67 observed [$I > 2\sigma(I)$], 7 parameters.

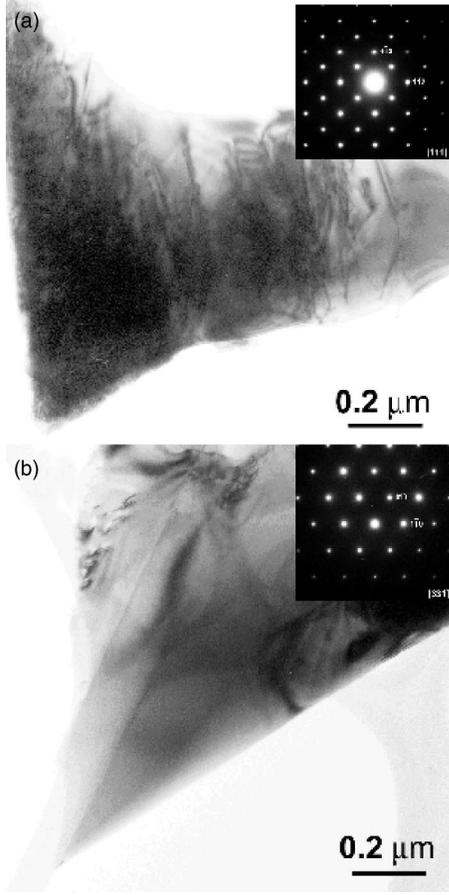| Atom	x	y	z	U_{iso}
Yb	0	0	0	0.0052(6)
Ni	0	0.5	0.25	0.0042(6)
B	0	0.5	0.361(2)	0.0044(4)
C	0.5	0.5	0	0.0065(4)

FIG. 5. Bright-field TEM image of the crush-made as-grown (a) and annealed (b) YbNi$_2$B$_2$C single grains. SAEDP is shown as inset.

Kondo impurity for $T \ll T_K$ (Kondo temperature associated with the impurity) can be written as[9,24]

$$\Delta\rho_{max} = \frac{\hbar}{e^2} \frac{4\pi c}{p k_F} (2l+1),$$

where in our case c is the fraction of Yb sites affected by disorder, k_F is the Fermi momentum, p is the number of electrons per atom, and l is the ytterbium $4f$ angular momentum. Using this expression we estimated an increase in the room temperature resistivity of ~ 30 $\mu\Omega$ cm for a 1% concentration of Yb sites with T_K greater than 300 K. The extended resistivity measurements and analysis performed in the present work have confirmed and reinforced that initially proposed semiquantitative model. We have observed that when the sample is well into the coherent scattering regime ($T \ll T_K \sim 10$ K) or well above the maximum perturbed Kondo temperature ($T \gg T_K^{max} \sim 600$ K) the Yb ions behave like the more conventional, nonhybridizing rare-earth members in the RNi$_2$B$_2$C series and the overall resistivity decrease with annealing is of only 2–3 $\mu\Omega$ cm, once again consistent with a density of order 1% of conventional scattering sites.

The TEM experiments clearly showed the presence of defects in both unannealed and annealed samples most likely associated with lattice dislocations, and the defect density was estimated to be *at least* 2.5 times larger in the unannealed samples. Similar qualitative changes were seen in the XRD data. With these results we can propose a scenario where the dislocation sites act as a source of strain fields which disturb nearby Yb sites with intensity inversely proportional to their distance to the defect origin, which would then lead to the appearance of a distribution of local Kondo temperatures along the strain field decay. Estimating the extension of a strain field around a dislocation core is complicated, and will vary according to the nature of the dislocation, the modulii of the material and the length of the Burger's vector. However, we can once again attempt a semi-quantitative analysis. Using the defect density of 1.5 $\times 10^8$ cm^{-2} for the unannealed sample and assuming that 1% of the Yb sites are subject to a strain field, we can estimate that all Yb sites within a radius of 460 Å of each dislocation core would be feeling the effect of the strain field. This value corresponds to about 130 unit cells along the plane and 40 unit cells along the c axis, and seems rather large given that, according to Eshelby and others,[25] the region of elastic limit should be on the order of 5 times the Burger's vector. For our samples the dislocations appear to be of the $1/2\langle 110\rangle\{001\}$ type with corresponding Burger's vector $b = a/2[110] \approx 2.47$ Å. We can still argue an enhanced sensitivity of the hybridized Yb ions to the strain, but even so it is likely that the extension of the strain field (or the fraction of affected Yb sites) is being overestimated.

Whereas there are very clear changes in the microstructural data (TEM and single-crystal XRD) with annealing, the link between these changes and the changes in the transport measurements remains only semiquantitative.

VII. CONCLUSION

In this work we have fully characterized the resistivity behavior of annealed and unannealed YbNi$_2$B$_2$C single crystals in the range of $0.4 < T < 1000$ K. Whereas the variability of resistivity behavior for compounds with hybridizing moments has been long suspected, our studies on YbNi$_2$B$_2$C finally allow a clear and controlled demonstration of this effect. We were also able to use single crystal XRD and TEM data to gain confidence in the claim that the changes are indeed intrinsic to the compound which is clearly single phase in both annealed and as-grown conditions. For this particular material and growth process, lattice dislocations seem to be the dominant defect type found in as-grown crystals, and is most likely being responsible for environment changes in the nearby Yb^{3+} ions which lead to deviations of local Kondo temperatures from their intrinsic value of ~ 10 K. As a consequence, it is important to realize that any attempt at detailed analysis of transport properties such as those found for YbNi$_2$B$_2$C (and these are not uncommon) are highly suspect, and any comparison of experiments with theoretical models must either take into account the sensitivity of the hybridizing moments on the modelling side or guarantee a nearly defect-free sample, a highly nontrivial experimental requirement.

[1] G.R. Stewart, Rev. Mod. Phys. **56**, 755 (1984).

[2] W. Franz, A. Griessel, F. Steglich, and D. Wohlleben, Z. Phys. B **31**, 7 (1978).

[3] A. Yatskar, N.K. Budraa, W.P. Beyermann, P.C. Canfield, and S.L. Bud'ko, Phys. Rev. B **54**, R3772 (1996).

[4] S.K. Dhar, R. Nagarajan, Z. Hossain, E. Tominez, C. Godart, L.C. Gupta, and R. Vijayaraghavan, Solid State Commun. **98**, 985 (1996).

[5] U. Grasser, P. Allenspach, F. Fauth, W. Henggeler, J. Mesot, A. Furrer, S. Rosenkranz, P. Vorderwisch, and M. Buchgeister, Z. Phys. B: Condens. Matter **101**, 345 (1996).

[6] M. Rams, K. Krolas, P. Bonville, J.A. Hodges, Z. Hossain, R. Nagarajan, S.K. Dhar, L.C. Gupta, E. Alleno, and C. Godart, J. Magn. Magn. Mater. **219**, 15 (2000).

[7] A.T. Boothroyd, J.P. Barratt, P. Bonville, P.C. Canfield, A. Murani, A.R. Wildes, and R.I. Bewley, Phys. Rev. B **67**, 104407 (2003).

[8] X.Y. Miao, S.L. Bud'ko, and P.C. Canfield, J. Alloys Compd. **338**, 13 (2002).

[9] M.A. Avila, S.L. Bud'ko, and P.C. Canfield, Phys. Rev. B **66**, 132504 (2002).

[10] P.C. Canfield, P.L. Gammel, and D.J. Bishop, Phys. Today **51**, 40 (1998).

[11] G.M. Sheldrick, *SHELXTL, version 6.10* (Bruker AXS Inc., Madison, WI, 2000).

[12] S.L. Bud'ko, P.C. Canfield, A. Yatskar, and W.P. Beyermann, Physica B **230-232**, 859 (1997).

[13] Z. Hossain, R. Nagarajan, S.M. Pattalwar, S.K. Dhar, L.C. Gupta, and C. Godart, Physica B **230-232**, 865 (1997).

[14] A. Yatskar, C.H. Mielke, P.C. Canfield, A.H. Lacerda, and W.P. Beyermann, Phys. Rev. B **60**, 8012 (1999).

[15] K.D.D. Rathnayaka, D.G. Naugle, S. Lim, M.C. de Andrade, R.P. Dickey, A. Amann, M.B. Maple, S.L. Bud'ko, P.C. Canfield, and W.P. Beyermann, Int. J. Mod. Phys. B **13**, 3725 (1997).

[16] K.O. Cheon, I.R. Fisher, V.G. Kogan, P.C. Canfield, P. Miranovic, and P.L. Gammel, Phys. Rev. B **58**, 6463 (1998).

[17] A. Yatskar, S.L. Bud'ko, P.C. Canfield, W.P. Beyermann, G.M. Schmiedeshoff, M.S. Torikachvili, C.H. Mielke, and A. Lacerda, Physica B **230-232**, 876 (1997).

[18] K. Kadowaki and S.B. Woods, Solid State Commun. **58**, 507 (1986).

[19] N. Tsujii, K. Yoshimura, and K. Kosuge, J. Phys.: Condens. Matter **15**, 1993 (2003).

[20] X. Y. Miao, S. L. Bud'ko, and P. C. Canfield (unpublished results related to Ref. 8).

[21] T. Siegrist, H.W. Zandbergen, R.J. Cava, J.J. Krajewski, and W.F. Peck, Nature (London) **367**, 146 (1994).

[22] T. Siegrist, R.J. Cava, J.J. Krajewski, and W.F. Peck, J. Alloys Compd. **216**, 135 (1994).

[23] L. Beraha, M. Duneau, H. Klein, and M. Audier, Philos. Mag. A **76**, 587 (1997).

[24] J.D. Thompson and Z. Fisk, Phys. Rev. B **31**, 389 (1985).

[25] P.B. Hirsch, *The Physics of Metals* (Cambridge University Press, Cambridge, England, 1975), Vol. 2, p. 302.